Bioresource Technology 437 (2025) 133150

Contents lists available at ScienceDirect

Bioresource Technology

journal homepage: www.elsevier.com/locate/biortech

Optimizing butyrate production from methanol and CO_2 in microbial electrosynthesis

Hui Yao [a], Paolo Dessì [c], Meritxell Romans-Casas [b], Sebastià Puig [b], Marika Kokko [a,*]

[a] Faculty of Engineering and Natural Sciences, Tampere University, Korkeakoulunkatu 8, 33720 Tampere, Finland
[b] LEQUiA, Institute of the Environment, University of Girona, Campus Montilivi, C/Maria Aurèlia Capmany, 69, Girona 17003, Spain
[c] Department of Agricultural Sciences, University of Naples Federico II, Piazza Carlo di Borbone 1, 80055 Portici, Italy

HIGHLIGHTS

- $MeOH/CO_2$ ratios, temperatures and gas pressures were optimized in gas fermentation.
- Butyrate production was ceased at 23 °C.
- Optimal butyrate production obtained at 35 °C, 3:1 $MeOH/CO_2$ ratio, and 1 atm.
- Optimal scenario was validated in MES: butyrate production rate of 107 g m^{-2} d^{-1}.
- 3:1 $MeOH/CO_2$ ratio enhanced the methanol utilization rate.

GRAPHICAL ABSTRACT

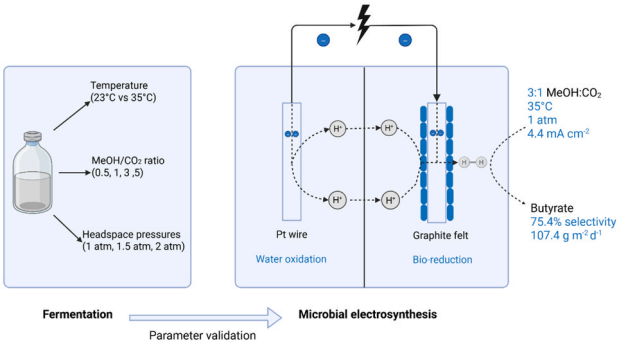

ARTICLE INFO

Keywords:
Microbial electrosynthesis
Butyrate
Methanol
Carbon dioxide
Process optimization

ABSTRACT

Microbial electrosynthesis (MES) enables the conversion of carbon dioxide (CO_2) into valuable chemicals utilizing renewable electricity. Acetate is often the main product but supplying a soluble electron donor facilitates upgrading acetate to butyrate via chain elongation. Compared to ethanol as the electron donor, methanol is a promising alternative as its production avoids the competition with food production. However, the optimal operation conditions for maximizing butyrate production rates in methanol assisted MES have not yet been determined. In this study, methanol assisted chain elongation process was first evaluated in batch bottles to set up the optimal scenario for butyrate production. The highest butyrate production rates and titers were achieved at 35 °C temperature, 1 atm headspace pressure, and a methanol/CO_2 ratio of 3 (on a carbon basis). These operational conditions were subsequently applied to a MES cell operated in fed-batch mode, obtaining a remarkable average butyrate production rate of 107.4 ± 19.7 g m^{-2} d^{-1} and a selectivity of 75.2 ± 1.1 %. In particular, temperature was a pivotal factor determining butyrate productivity. At 23 °C, regardless of changes in pressure or methanol/CO_2 ratio, acetate remained the main product (with selectivity over 80 %) in both fermentation batch bottles and in MES. In conclusion, this study not only provided a comprehensive multivariable analysis to optimize key operational parameters for methanol assisted chain elongation but also demonstrated an effective strategy for butyrate production from CO_2 and methanol in MES.

* Corresponding author.
E-mail address: marika.kokko@tuni.fi (M. Kokko).

https://doi.org/10.1016/j.biortech.2025.133150
Received 13 June 2025; Received in revised form 11 August 2025; Accepted 11 August 2025
Available online 13 August 2025

1. Introduction

Carbon dioxide (CO_2) can be seen as a critical feedstock for producing a plethora of commodities, such as biofuels and platform chemicals offering a pathway towards carbon neutrality (Appel et al., 2013). Among the existing CO_2 conversion routes, the Wood-Ljungdahl pathway (WLP) is the most ancient and energetically favorable, considering the net adenosine triphosphate (ATP) input (Zhao et al., 2021). In WLP, acetogenic bacteria reduce CO_2 into biochemicals using hydrogen (H_2) as an electron donor (Ragsdale and Pierce, 2008), and resulting in the formation of acetyl-CoA, which can be further converted to acetate (Eq. (1)) or reduced to valuable compounds (Ragsdale and Pierce, 2008).

$$2CO_2 + 4H_2 \rightarrow CH_3COO^- + H^+ + 2H_2O \quad (1)$$

Several biological processes have employed acetogenic bacteria for the biochemical production from CO_2. For example, gas fermentation is a process where microorganisms convert gaseous substrates (carbon monoxide (CO), CO_2 and H_2) into biochemicals. However, the gas fermentation kinetics are limited by mass transfer of gases to the liquid phase (Ale Enriquez and Ahring, 2023). An alternative biological CO_2 fixation method is microbial electrosynthesis (MES). In MES, acetogens are cultivated in an electrochemical cell by utilizing electrons from a cathode electrode as reducing power (Nevin et al., 2010). In situ produced H_2 at the cathode serves as the electron donor for acetogens to reduce CO_2 via the WLP, with acetate being often the primary product (Jourdin and Burdyny, 2021).

In MES, additional electron donors could facilitate the chain elongation process and yielding spectrum of products including short to medium-chain carboxylic acids (Izadi et al., 2021; Romans-Casas et al., 2024; Vassilev et al., 2018). The most common electron donor in MES is ethanol, which shifts the production from acetate to butyrate (Vassilev et al., 2019), butanol (Romans-Casas et al., 2024), and caproate (Jiang et al., 2020). However, the current ethanol production is mainly crop-based and raises concerns between food and fuels competition (Joyia et al., 2024). Methanol can be a great substitute for ethanol as electron donor for chain elongation. Currently, methanol is primarily produced from natural gas-derived syngas, with an annual global production of approximately 110 million metric tons, making it a low-cost and well established feedstock chemical (Tabibian and Sharifzadeh, 2023). Moreover, methanol can potentially be synthesized from biomass-derived gases (Varela et al., 2024) or directly from CO_2 via electrochemical routes (Lee et al., 2024), though the electrochemical methanol synthesis from CO_2 is still in the early stages of development and primarily limited to laboratory-scale applications (Li et al., 2024a). In bioproduction processes, the utilization of methanol has been extensively explored since the 1970 s (Taylor and Senior, 1978), and anaerobic methylotrophic archaea and acetogenic bacteria have been widely reported for natural methanol assimilation (Kremp and Müller, 2021). For example, *Eubacterium limosum* is a well-known bacteria for methanol assimilation, starting by transferring the methyl group of methanol to tetrahydrofolate (THF), which is further reduced via the WLP, releasing reducing equivalents that not only promote the production of acetate (Eq. (2)), but also the production of butyrate (Eq. (3)), butanol and caproate (Kremp and Müller, 2021; Wood et al., 2022). Therefore, methanol was used by mixed cultures to conduct the chain elongation process from acetate for butyrate, isobutyrate and caproate production by utilizing the reducing power of methanol (Chen et al., 2017, 2016; De Leeuw et al., 2020). Moreover, the addition of methanol has been shown to enhance performance of both gas fermentation and MES processes (Kim et al., 2021; Yao et al., 2024). In gas fermentation, adding methanol along with H_2/CO_2 boosted the microbial growth rates by four-fold and the H_2 consumption rate by 2.7-fold (Yasin et al., 2015). The addition of methanol along with CO_2 in MES shifted the product spectrum from acetate towards butyrate (82 % selectivity), resulting in 1.8-fold higher production rates and 1.7-fold higher titer than using CO_2 as the sole substrate (Yao et al., 2024).

$$4CH_3OH + 2HCO_3^- \rightarrow 3CH_3COO^- + 4H_2O + H^+ \quad (2)$$

$$2CH_3OH + CH_3COO^- \rightarrow CH_3(CH_2)_2COO^- + 2H_2O \quad (3)$$

In this study, methanol was chosen as the electron donor not only for its metabolic compatibility with *E. limosum*, but also due to its lower cost and the non-competition with food resources. The *Eubacterium*-dominated microbiome was not selected, but has been continuously enriched in over three-years cultivations when fed only with methanol and CO_2. Although methanol has shown potential to enhance the performance of MES, operational parameters remain underexplored in methanol assisted MES. So far, only the cathodic pH has been optimized, obtaining a selective butyrate production (87 % selectivity) at pH 6 (Yao et al., 2025). Other operational parameters including temperature, headspace pressure, and methanol/CO_2 ratio could also potentially affect the methanol assisted MES. Acetogenic bacteria are generally grown in mesophilic conditions and thus most of the MES studies have been conducted between 20 ℃ to 37 ℃ (Yang et al., 2018). Within this range, temperature can also affect the MES performance. For example, a mixed culture study carried out by Yang et al. (2021) compared the performance of CO_2-fed MES from 10 ℃ to 70 ℃, which showed a slightly higher acetate titer of 525.8 ± 1.5 mg L^{-1} at 25 °C compared to the titer of 468.5 ± 7.1 mg L^{-1} at 35 °C, yet a higher acetate production rate at 35 °C (49.2 ± 0.5 mg $L^{-1}d^{-1}$) compared to 25 °C (25.3 ± 1.5 mg $L^{-1}d^{-1}$) (Yang et al., 2021). Specifically, the experimental temperatures of 23 °C and 35 °C were interesting based on prior studies and practical considerations. While 37 °C is reported as the optimal growth temperature for *E. limosum*, 35 °C has been widely used in both pure culture studies (Flaiz et al., 2024; Shin et al., 2023) and mixed-culture methanol-based chain elongation and MES systems (Chen et al., 2017; De Smit et al., 2019; Rode et al., 1981). On the other hand, 23 °C was chosen to evaluate system performance under room temperature conditions, offering insights relevant to scale-up and environmental variability. The partial pressures of H_2 (P_{H2}) and CO_2 (P_{CO2}) are other key parameters that affect microbial metabolism and bioproduction in both gas fermentation and MES (Romans-Casas et al., 2024; Skidmore et al., 2013; Yerushalmi et al., 1985). For instance, increasing the headspace pressure in gas fermentation has been shown to improve the gas to liquid mass transfer and thus improve the overall production and biomass growth (Oswald et al., 2018; Van Hecke et al., 2019). In MES, sustaining a P_{CO2} of 1.5 atm by daily replenishment was an efficient strategy to promote selective butyrate production (bringing to a 78 % selectivity on a carbon basis) with CO_2 as the only carbon source (Romans-Casas et al., 2024). Lastly, the methanol/CO_2 ratios could also potentially affect the product spectrum. High ratios could promote production of more reduced products over acetate. As reported in a fermentation study by Wood et al., (2022) increasing the methanol to formate ratio above five (mol/mol) induced the production of butanol by *E. limosum*. Although the influence of the aforementioned process parameters could offer valuable insights into the role of methanol and its potential to enhance butyrate production, these factors have, to the best of our knowledge, not been extensively explored within the context of methanol-assisted gas fermentation and microbial electrosynthesis (MES) processes.

Therefore, this study investigated the effects of key operational parameters — temperature, methanol/CO_2 ratios, and headspace partial pressures — on methanol assisted MES as a basis for process optimization in terms of production rates, titers and selectivity. Various combinations of these operational parameters were first tested under gas fermentation conditions in serum flasks fed with methanol and H_2/CO_2. The obtained results were subsequently validated in MES reactors operating in fed-batch mode and fed with methanol and CO_2 providing insights for further steps in process intensification.

2. Materials and methods

2.1. Inoculum and medium

An *Eubacterium* sp. dominated mixed culture was obtained from the cathodic chamber of a MES reactor (Yao et al., 2024) and used as the inoculum in this study. The catholyte from the inoculum reactor was added to the fresh biological medium with a 1:10 (v/v) ratio to start the experiments. The medium was a phosphate buffered biological medium prepared by following the recipe in the supplementary information. Before the inoculation, N_2 was sparged through the medium to eliminate dissolved oxygen.

2.2. Fermentation in serum flasks

The working volume of the serum flask was 40 mL, with an 80 mL headspace volume. The effect of operational parameters on fermentative carboxylate production from methanol, CO_2 and H_2 were tested in serum flasks in duplicate for seven days (Table 1). Parameters of interest included temperature, methanol/CO_2 feeding ratios, P_{H2} and P_{CO2}. The initial pH of the fermentation broth was set at 7.2 for all conditions. The flasks were sealed and placed under agitation at 120 rpm at either room temperature (23 °C) or in a temperature-controlled incubator (35 °C). Different initial methanol/CO_2 ratios (from 0.5 to 5) were set by supplementing methanol from a stock solution (0.2 to 2.3 mol L^{-1}), every two to three days for a total of three additions. A gas mixture of 80 % H_2 and 20 % CO_2 was used to sparge the flasks and then to apply pressures of either 1, 1.5 or 2 atm. Both liquid and gas samples were collected daily, accompanied with sparging the serum flasks for three minutes and regulating the headspace pressures via a gas manometer (Leo1 Keller, Switzerland).

2.3. MES reactor set-up and operation

Based on fermentation experiment results, two different operational parameter combinations were evaluated with the aim of achieving selective production of butyrate or acetate in methanol-assisted MES. One combination (35 °C, atmospheric pressure, and methanol/CO_2 ratio of 3) was aiming for optimal butyrate production (MES-35). Another combination (23 °C, maximum overpressure of 1.5 atm and ratios ranging from 0.3 to 1) was aiming to achieve selective acetate production (MES-23). As proposed by Yao et al. (2025), the pH in the MES experiments was manually adjusted to above 6 using 3 mol L^{-1} NaOH when it fell below 6 to prevent potential inhibition of methanol utilization.

To maintain overpressure requirements, two commercial, pressurizable electrochemical cells (MicroFlowCell, ElectroCell, Denmark) were employed to conduct MES-23 experiments. Carbon felt (99 %, Fisher scientific, Spain) and a dimensionally stable electrode (DSA-O2) with projected surface areas of 10 cm^2 each were used as the cathode and anode, respectively. The working volumes of the cathode and anode chambers were 4 and 3 mL, respectively, separated by a reinforced cation exchange membrane (CEM, Nafion N324, USA) (Romans-Casas et al., 2024). Both the cathode and anode were connected to their respective recirculation bottles through recirculation lines using a peristaltic pump (Watson Marlow 205U, UK) with a flow rate of 5.2 mL min^{-1}. Anodic recirculation bottles were open to the ambient atmosphere, while the cathodic recirculation bottles were sealed to prevent gas leakage (headspace volume of 76 mL). The total volume of both catholyte and anolyte was 80 mL. A reference electrode (Ag/AgCl, +0.197 V vs. SHE, RE-5B, BASI, USA) was inserted into the anodic recirculation line.

The MES-23 experiments lasted for 70 days, during which CO_2 was sparged through the cathodic recirculation bottles for three minutes every two to three days, after which an initial P_{CO2} of 1.5 atm was set by closing the gas outlet. The cells were operated in two-electrode configuration and in galvanostatic mode by using a potentiostat (VSP, Bio-Logic, France). The applied current density was set to 1.5 mA cm^{-2} from days 0 to day 43, and 3.0 mA cm^{-2} from day 43 to day 70, while cell voltage was continuously monitored. The methanol addition ranged from 12 mmol per week to 2 mmol per week to maintain methanol/CO_2 ratios between 0.3 and 1.

As the MES-35 experiments did not require overpressure condition, a two-chamber flat-plate reactor was used, with a working volume of 23

Table 1
Operational parameters tested as fermentation process in shake flasks, and the results obtained for biomass growth (as OD_{600}), net production of acetate and butyrate, butyrate selectivity (S_B) and carbon conversion efficiency (CCE). All the runs were run as duplicates for seven days.

Operation conditions			Results				
T (°C)	p (atm)	Methanol/ CO_2 ratio	OD_{600} (nm)	Acetate produced (mmol-C)	Butyrate produced (mmol-C)	S_B (%)	CCE (%)
23	1	0.5	2.1 ± 0.2	3.09 ± 0.77	0.32 ± 0.32*	7.1 ± 7.1*	77.6 ± 4.3
		1	2.2 ± 0.4	2.66 ± 0.24	0.15 ± 0.15*	4.8 ± 4.8*	52.1 ± 3.9
		3	1.9 ± 0.2	3.99 ± 0.60	0.11 ± 0.11*	2.4 ± 2.4*	63.6 ± 7.8
		5	1.3 ± 0.2	2.45 ± 0.91	–	–	23.2 ± 11.3
	1.5	0.5	1.3 ± 0.1	3.93 ± 0.05	–	–	67.7 ± 4.4
		1	1.4 ± 0.2	2.87 ± 2.20	–	–	33.0 ± 22.5
		3	1.2 ± 0.2	3.76 ± 0.31	0.02 ± 0.02*	0.6 ± 0.6*	23.8 ± 4.6
		5	1.0 ± 0.3	3.03 ± 0.27	–	–	22.4 ± 5.2
	2	0.5	2.2 ± 0.1	5.42 ± 0.24	0.10 ± 0.03	1.8 ± 0.6	61.6 ± 0.8
		1	0.8 ± 0.0	2.69 ± 0.53	–	–	40.8 ± 2.3
		3	2.3 ± 0.1	5.75 ± 0.12	0.08 ± 0.06	1.5 ± 1	27.7 ± 1.9
		5	2.4 ± 0.0	5.95 ± 0.30	0.12 ± 0.04	2.0 ± 0.6	18.2 ± 1.7
35	1	0.5	2.3 ± 0.4	3.79 ± 0.03	0.81 ± 0.20	17.5 ± 3.5	96.1 ± 13.1
		1	3.4 ± 0.5	2.94 ± 1.03	1.03 ± 0.31	25.5 ± 6.1	58.3 ± 9.2
		3	3.0 ± 0.4	3.11 ± 2.61	2.61 ± 0.09	45.7 ± 3.7	62.5 ± 0.8
		5	2.4 ± 0.3	2.82 ± 2.42	2.42 ± 0.38	46.0 ± 5.5	46.3 ± 10.1
	1.5	0.5	2.6 ± 0.3	3.30 ± 0.27	2.53 ± 0.13	43.4 ± 0.7	56.5 ± 3.5
		1	3.0 ± 0.0	3.88 ± 0.86	3.10 ± 0.22	45.0 ± 3.8	52.1 ± 2.2
		3	2.7 ± 0.3	3.61 ± 0.33	3.45 ± 0.33	48.9 ± 0.1	32.3 ± 4.1
		5	2.8 ± 0.1	4.31 ± 0.20	3.16 ± 0.30	42.2 ± 1.2	27.4 ± 1.1
	2	0.5	2.0 ± 0.1	6.23 ± 0.21	1.29 ± 0.52	16.9 ± 6.2	61.9 ± 0.4
		1	2.6 ± 0.0	5.48 ± 0.24	1.82 ± 0.27	25.0 ± 3.6	45.3 ± 2.7
		3	3.5 ± 0.1	5.17 ± 0.34	2.21 ± 0.35	29.7 ± 2.0	33.1 ± 0.6
		5	2.9 ± 0.03	3.93 ± 0.59	2.51 ± 1.62	35.8 ± 19.4	20.7 ± 5.1

Symbol * denotes only one of the duplicates produced butyrate.

mL in each chamber. The chambers were separated by a cation exchange membrane (CXM-200, Membrane International, USA), with an active surface area of 20 cm^2. The cell was operated under galvanostatic mode, controlled by a potentiostat (VMP3, BioLogic, France). A platinum wire (0.4 mm, 99.95 %, Advent Research Materials, UK) was used as the anode electrode. Graphite felt (99.9 %, Thermo Scientific, USA) was pierced by stainless steel wire (current collector) and placed in the center of the cathodic chamber as the cathode (projected surface area of 20 cm^2). The electrodes and membrane were placed tightly to reduce energy losses due to internal resistance. A reference electrode (SE11NSK7, Sensortechnik Meinsberg, Germany) was integrated into the cathodic recirculation line close to the outlet (ca. 10 cm) of the cathode chamber via a sealed glass vial. The total volume of catholyte and anolyte were 360 mL and 200 mL, respectively. Each chamber was connected to a recirculation bottle, and the electrolytes were circulated at a flow rate of 40 mL min^{-1} (Masterflex L/S Digital Drive pump). The cathodic recirculation bottle was connected to a gas bag to prevent overpressures and collect gases, while the anodic recirculation bottles were open to ambient conditions.

The MES-35 experiments lasted for 30 days, with gas sparging, methanol addition, and sampling occurring three times a week. In order to obtain the 80 % H_2 and 20 % CO_2 headspace gas composition during each fed-batch cycle, the cell was operated at a current of −87 mA (4.4 mA cm^{-2}), and CO_2 was sparged through the cathodic recirculation bottles and collected in the gas bags for ten minutes at a flow rate of 50 mL min^{-1} (F-201CV, Bronkhorst, the Netherlands). The experiments were initiated by adding 180 mM methanol to the cell, and methanol concentration was maintained at 120 mM for two days and 180 mM for the following three days to achieve a target dosing rate of 60 mM d^{-1}, thereby sustaining a 3:1 methanol/CO_2 ratio (carbon basis) in each fed-batch cycle. Residual methanol concentration in the catholyte was measured before CO_2 sparging, and the required amount was manually added to adjust the concentration accordingly. Both liquid and gas samples were collected every two to three days.

2.4. Analyses and calculations

Gas and liquid samples were taken two to three days per week. Gas pressure was measured with a pressure meter (differential pressure gauge, Testo 512, Spain). Gas composition was analyzed by a gas chromatograph equipped with a thermal conductivity detector (GC-TCD, Shimadzu, Japan) and Agilent J&W packed GC column (2.00 mm internal diameter, 1.8 m length) or another GC-TCD (Micro GC 490, Agilent Technologies, USA) with two columns: a CP-Molesieve 5A column, and a CP-Poraplot U column. When using gas bags, the gas amount was quantified by the water displacement method to measure the gas volume inside the bags. The headspace pressure and volume were used for calculating gas volumes in fermentation and MES-23 experiments. Liquid samples (3 mL) were taken from both cathodic and anodic recirculation bottles in MES three times a week or daily for fermentation experiments, and analyzed for pH, optical density (OD), and the organics. The pH and OD_{600} were measured with a pH meter (Basic 20+, Crison Instruments, Spain or pH 3320, WTW, Germany) and a spectrophotometer (DR3900, Hach, Germany or UV-1800, Shimadzu, Japan), respectively. The remaining samples were filtered (0.2 μm) and analyzed by GC equipped with a flame ionization detector (GC-FID, GC 7890 A, Agilent Technologies, USA) using a DB-FFAP column or a GC-FID (GC-2010, Shimadzu, Japan) with a Zebron column (ZB-WAX plus, 0.25 μm diameter, 30 m length). Further details can be found in Romans-Casas et al., (2024) and in Yao et al., (2024), respectively.

The *selectivity* of the compound *i* was calculated according to Eq. (4):

$$\boldsymbol{Selectivity}_i = \frac{\boldsymbol{n}_i}{\boldsymbol{n}_{sum}} \times 100 \tag{4}$$

where selectivity of compound *i* is defined as the ratio of amount of compound n_i and the total amount of organic products n_{sum} in mol-C.

The yield of the compound *i* was calculated with Eq. (5):

$$\boldsymbol{Yield}_i = \frac{\boldsymbol{n}_i}{\boldsymbol{n}_{(carbondioxide)} + \boldsymbol{n}_{(methanol)}} \tag{5}$$

where n_i is the amount of compound *i* in mol-C, $n_{(carbon\ dioxide)}$ and $n_{(methanol)}$ are the amounts of consumed CO_2 and methanol in mol-C, respectively.

The faradaic efficiency (FE) of the compound *i* was calculated according to Eq. (6):

$$\boldsymbol{FE}_i = \frac{\boldsymbol{F} \times \boldsymbol{n}_i \times \boldsymbol{z}_i}{\int \boldsymbol{Idt} + \boldsymbol{F} \times \boldsymbol{n}_{Me} \times \boldsymbol{z}_{ME}} \times 100 \tag{6}$$

where FE_i is defined as the ratio of electrons transferred to product *i* and the total electrons provided, z_i represent the number of electrons transferred to each molecule of the the product *i*. *F* is faradaýs constant (96485C mol^{-1} electron), *n* is the amount of product *i* (mol), and *I* dt is the current consumed along the considered time (Ah).

The total carbon conversion efficiency (CCE) was calculated according to the following Eq. (7):

$$CCE = \frac{\boldsymbol{n}_{(VFAs)}}{\boldsymbol{n}_{(carbondioxide)} + \boldsymbol{n}_{(methanol,t1)}} \times 100 \tag{7}$$

where $n_{(VFAs)}$ is the sum of amounts of produced VFAs in mol-C, $n_{(carbon\ dioxide)}$ and $n_{(methanol)}$ are the amounts of consumed CO_2 and methanol in mol-C, respectively.

Obtained results were compared to test the significance of the differences obtained from different conditions. was assessed by using *t*-test or one-way analysis of variance (ANOVA) Post Hoc test, where the $p < 0.05$ was recognized as significant. The data was analyzed using ANOVA without the exclusion of outliers. Outliers were identified visually via box plots. The robustness of ANOVA ensured that the analysis remains valid even in the presence of these extreme values. The analyses were carried out in Origin 2024b.

3. Results and discussions

3.1. Methanol and H_2/CO_2 fermentation with different combinations of operational parameters

The fermentation experiments tested 24 different scenarios including different combinations of temperature (23℃ and 35℃), headspace pressure (1, 1.5, and 2 atm), and methanol/CO_2 ratios (0.5, 1, 3 and 5). A summary of the operational parameters and results is shown in Table 1.

3.1.1. VFA production at different temperatures

Acetate and butyrate were the two main products obtained in all fermentation experiments. Values represented correspond to net productions, calculated considering the concentrations measured at the end of each fermentation experiment. At room temperature, acetate was the dominant product, with amounts ranging between 2.5 and 6.0 mmol-C (Fig. 1.a). Meanwhile, only trace amounts of butyrate were produced with a titer not exceeding 0.32 mmol-C (Fig. 1.b). Thus, butyrate selectivity (S_B) under room temperature was below 10 % for every scenario (Table 1). At 35℃, acetate production was in the same range as at 23 ℃ (2.7–6.2 mmol-C) and no statistically significant difference was observed ($p > 0.05$). This range reflects the values observed across different methanol/CO_2 ratios and pressure conditions tested at 35 °C, while the corresponding average values for each condition are listed in Table 1. However, butyrate production was significantly higher at 35℃ than at 23℃. Butyrate accumulated to a titer of 0.8–3.5 mmol-C with selectivity ranging between 16.9 and 48.9 % (Table 1).

A similar trend has been observed with ethanol assisted chain elongation. A study carried out by Ren et al., (2024) compared chain

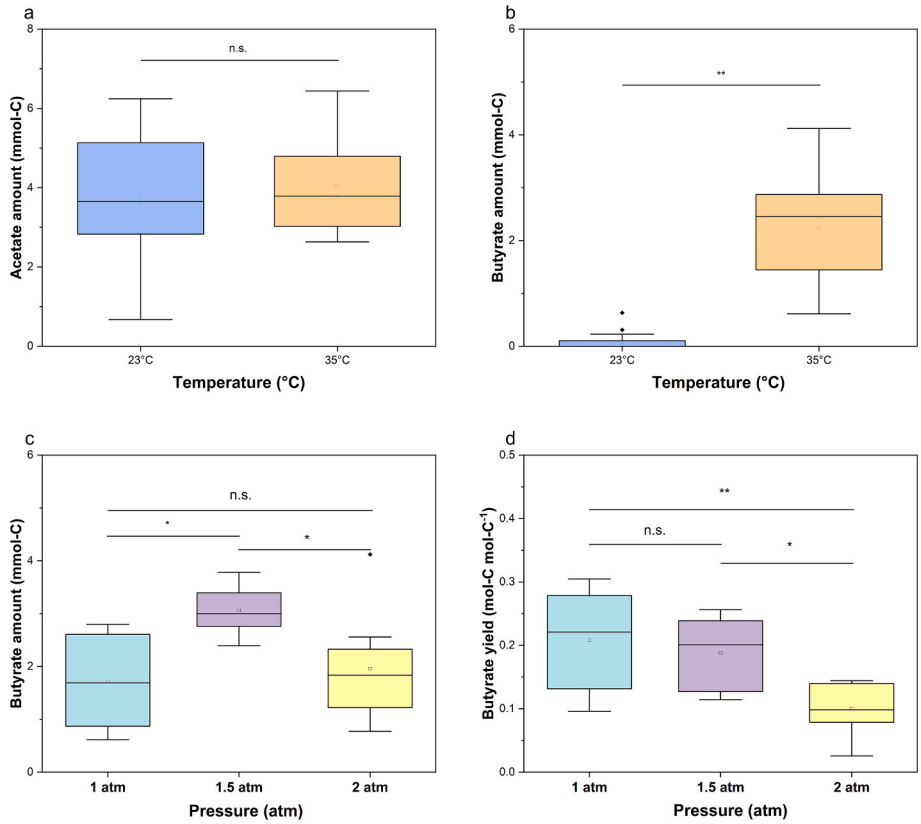

Fig. 1. Acetate (a) and butyrate production (b) at different temperatures, including results obtained at different pressure (1, 1.5 and 2 atm) and methanol/CO_2 ratio (0.5, 1, 3, and 5). Significance of results was tested by ANOVA and *t*-test. Butyrate amounts (c) and butyrate yields (d) at different pressures in fermentation experiments at 35 °C. The symbol * represents $p < 0.05$, symbol ** represents $p < 0.005$, symbol n.s. represents not significant.

elongation from ethanol and acetate between 25 and 55 °C, obtaining the highest caproate yield and selectivity at 40 °C. In contrast, the lowest caproate yield was obtained at 25 and 30 °C, where acetate production was stimulated (Ren et al., 2024). A reason for such difference was the composition of the microbial communities, as the key chain elongator, *Clostridium kluyveri*, was mostly enriched at 40 °C (Ren et al., 2024). Similarly, the dominant species in the inoculum used in this study, *E. limosum*, likely responsible for methanol utilization and butyrate production (Yao et al., 2025), has the optimal growth temperature at 37 °C (Rode et al., 1981).

3.1.2. VFA production at different pressures

As butyrate production mainly occurred at 35 °C, the effects of headspace pressures on butyrate production are discussed at that temperature (Fig. 1.c). As different substrate ratios (0.5, 1, 3, and 5) were used, a total of eight results were obtained for each pressure. Higher butyrate amounts, in the range of 2.4–3.8 mmol-C, were obtained at a headspace pressure of 1.5 atm. At 1 atm, butyrate amounts were in the range 0.6–2.8 mmol-C, while at 2 atm they were at 0.8–2.6 mmol-C, except at a methanol/CO_2 ratio of 5 where 4.1 mmol-C butyrate was obtained. In summary, butyrate productions were enhanced when the pressure was increased from 1 atm to 1.5 atm. Increasing the pressure enhances gas-to-liquid mass transfer and results in a higher solubility of gaseous compounds (according to Henry's law). Thus, the higher the P_{CO2}, the higher is the availability of soluble carbon sources. The butyrate yields (Fig. 1.d) were similar at 1 and 1.5 atm (0.15–0.29 and 0.12–0.25 mol-C mol-C^{-1}, respectively), both higher than the 0.08–0.11 mol-C mol-C^{-1} observed at 2 atm. Therefore, the higher butyrate amounts at 1.5 atm were likely due to the higher carbon availability compared to 1 atm, rather than a butyrate yield increase. Further increasing pressure (from 1.5 atm to 2 atm) resulted in higher biomass formation, as indicated by the increase in average OD_{600} from 2.0 to 2.4 (Table 1). However, both butyrate amount and yield decreased, suggesting that butyrate production was hindered.

On the other side, pressure increases also affected acetate production (see supplementary information). The highest acetate amount of 2.2–6.2 mmol-C was obtained at 2 atm. At pressures of 1 and 1.5 atm, acetate amounts decreased to 1.5–4.6 mmol-C and 0.7–5.1 mmol-C, respectively. The differences in acetate and butyrate production between 1.5 and 2 atm suggests elevated pressure may affect metabolism, potentially altering carbon fluxes. In addition to altering the product spectrum, microbial growth was also affected by the elevated pressures. Many studies have shown that the increased pressure resulted in higher biomass production (Gaddy, 1997; von Canstein et al., 2008; Wendlandt et al., 1993). However, the opposite effect has been observed as well, especially with higher pressure compared to values studied in this work. For instance, increasing the total pressure from 1 to 7 atm during cultivation with H_2/CO_2 gas mixtures led to a gradual decline in *C. ljungdahlii* biomass formation, likely resulting from the inhibitory effects of high P_{H2} (Oswald et al., 2018).

3.1.3. Butyrate production with different methanol/CO_2 ratios

Based on the results obtained, 35 °C and atmospheric headspace pressure were selected as the optimal conditions for evaluating butyrate production under various methanol/CO_2 ratios. Under such conditions, increasing the methanol/CO_2 ratio in the range 0.5 to 3 resulted in higher butyrate amounts (Table 1) and yields (Fig. 2). At a methanol/CO_2 ratio of 0.5, a relatively low butyrate amount of 0.8 ± 0.2 mmol-C and a yield of 0.17 ± 0.06 mol-C mol-C^{-1} were obtained. When the ratio was increased to 1, the butyrate amount increased to 1.0 ± 0.3 mmol-C with a yield of 0.15 ± 0.06 mol-C mol-C^{-1}. The highest butyrate production was obtained at a methanol/CO_2 ratio of 3, with the amount of

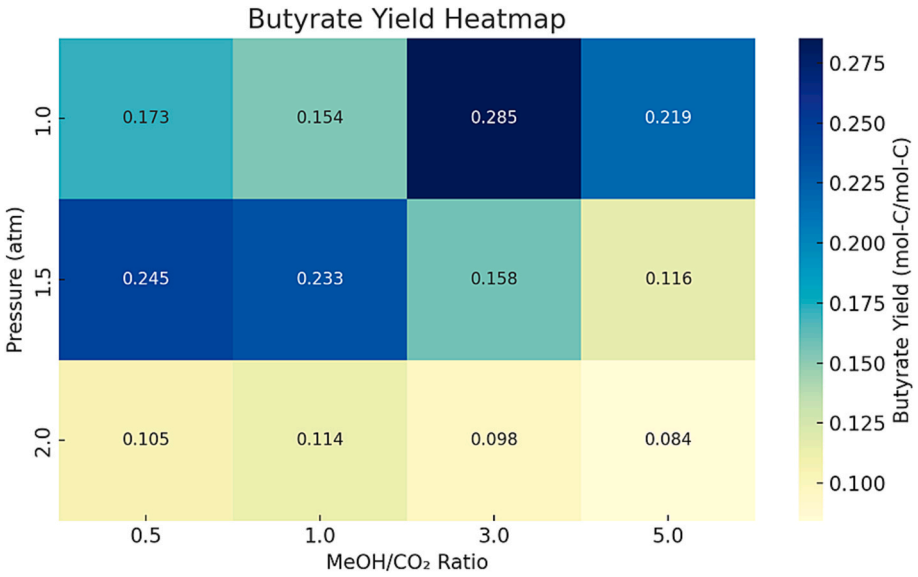

Fig. 2. Butyrate yield (mol-C mol-C^{-1}) at 35 °C at different pressure and methanol/CO_2 ratios.

2.6 ± 0.1 mmol-C and yield of 0.29 ± 0.02 mol-C mol-C^{-1}. However, increasing the ratio to 5 did not further increase the butyrate amount (2.4 ± 0.4 mmol-C) and resulted in a slightly lower yield of 0.22 ± 0.07 mol-C mol-C^{-1}. As Wood et al., (2022) suggested, a higher ratio of electron donor to electron acceptor promotes the synthesis of more reduced compounds in methanol assisted chain elongation. Therefore, increasing the ratio from 0.5 to 3 was expected to enhance butyrate production. However, a ratio of 5 led to methanol accumulation exceeding 250 mM, which could hinder the biomass growth and production efficiency (Kremp and Müller, 2021). According to Sharak Genthner and Bryant, (1987), methanol concentrations above 198 mM negatively affect *E. limosum* growth by increasing the doubling time and resulting in a lag phase of 79 h. To summarize, the optimal butyrate production was achieved at a temperature of 35 °C, atmospheric pressure, and a methanol/CO_2 ratio of 3.

3.2. Process validation in MES reactors

3.2.1. Acetate as the main product with pressurized conditions at 23°C

The first experiment in MES reactors aimed at testing methanol assisted MES under pressurized condition to target acetate production. Thus, based on the batch experiment results, room temperature (23 °C) was selected. As CO_2 was provided in overpressure, thereby increasing the solubilized CO_2 concentration, maintaining a high methanol/CO_2 ratio could lead to excessive methanol accumulation that could hinder microbial growth (Kremp and Müller, 2021). Thus, since no clear beneficial effect of high methanol/CO_2 ratios on the acetate productivity was observed in the incubation at 23 °C (Table 1), low methanol/CO_2 ratios (below 1) were used in this test. The two pressurized cells (MES-23-R1 and −R2) were initially operated at a constant current density of 1.5 mA cm^{-2} and an addition of 4 mmol methanol three times per week. The OD_{600} sharply increased from 0.04 to 0.17 on day 7 and remained between 0.15 and 0.2 until day 42 (see supplementary information). To maintain a methanol/CO_2 ratio below 1, only 2 mmol of methanol were added three time a week from day 7 to 26, resulting in a methanol/CO_2 ratio of ca. 0.9 ± 0.1 which enabled acetate production at rates up to 0.40 ± 0.04 g L^{-1} d^{-1} (37.5 ± 4.0 g m^{-2} d^{-1}) (Table 2). From day 26 onwards, methanol dosage was further decreased to 2 mmol per week, thus decreasing methanol/CO_2 ratio to 0.5 ± 0.3. The highest acetate titer of 5.8 ± 0.8 g L^{-1} was achieved on day 33 with a production rate of 0.47 ± 0.2 g L^{-1} d^{-1} (46.8 ± 18.3 g m^{-2} d^{-1}) in MES-23-R1. In MES-23-R2, 80 % of the catholyte was replaced with fresh medium on both days 26 and 35, which resulted in the highest acetate production rate of 0.7 g L^{-1} d^{-1} (69.4g m^{-2} d^{-1}) between days 35 to 42 (see supplementary information).

From day 42 onwards, the current density for both MES cells was increased to 3.0 mA cm^{-2}, resulting in higher H_2 accumulation at the end of each batch cycle (pressure increased from ca. 0.8 atm to 1.2 atm). This led to a higher microbial growth resulting in an OD_{600} increase from 0.15 to 0.26 (Table 2). This observation was in line with the results from gas fermentation experiments, in which higher microbial growth was obtained when applying higher overpressures. The acetate titer increased to 8.5 ± 1.1 g L^{-1} while the acetate production rates remained at 0.41 ± 0.04 g L^{-1} d^{-1} (41.2 ± 3.5g m^{-2} d^{-1}). In addition to acetate, butyrate production was observed throughout the experiments, yet with a low production rate (below 0.01 g L^{-1} d^{-1}) resulting in a titer of only 0.6 ± 0.1 g L^{-1}. Butyrate production was not affected by changes in either the applied current or methanol/CO_2 ratio.

One of the putative causes for the hindered butyrate production was the insufficient methanol utilization. In the MES experiments, methanol

Table 2
Operational conditions and key performance results for MES-23 reactors.

Main Product	Production period (days)	Current density (mA cm^{-2})	Methanol addition (mmol/ week)	MeOH/CO_2 ratio	Final OD_{600} (nm)	Production rate		Titer (g L^{-1})
						mg L^{-1}d^{-1}	g m^{-2} d^{-1}	
Acetate	9–19 (R1) 14–21(R2)	1.5	6.0	0.9 ± 0.1	0.15 ± 0.01	374.8 ± 39.7	37.5 ± 4.0	5.0 ± 0.3
	26–33 (R1,R2) 35–42 (R2)	1.5	2.0	0.5 ± 0.3	0.18 ± 0.01	467.6 ± 182.7	46.8 ± 18.3	5.6 ± 0.8
	44–51 (R1) 42–47 (R2)	3.0	2.0	0.3 ± 0.1	0.26 ± 0.01	412.7 ± 35.8	41.3 ± 3.6	8.5 ± 1.1

was utilized at an average rate of 0.17 g L^{-1} d^{-1}, while a methanol utilization rate of 0.32 g L^{-1} d^{-1} was obtained in previous experiments in MES at 35 °C (Yao et al., 2024). A carbon conversion efficiency (CCE) of 17.9 ± 1.7 % was obtained throughout the MES-23 runs, indicating that most of the carbon was not recovered in the products. Several factors likely resulted in the low CCE. For example, although the reactor itself was designed to handle pressurized condition, the membrane was not optimized for pressurized conditions, which likely resulted in the leakage of CO_2 and methanol (Fang et al., 2024; Koskue et al., 2021).

3.2.2. *MES optimization for efficient butyrate production*

Based on the results from gas fermentation (section 3.1), complementary MES experiments (MES-35) were conducted at 35℃ and atmospheric pressure setting methanol/CO_2 ratio of 3 aiming for selective butyrate production (Fig. 3). Acetate production initiated immediately after inoculating the reactors, with a production rate of 0.2 ± 0.1 g L^{-1} d^{-1} reaching a highest acetate titer of 5.6 ± 1.0 g L^{-1}. Butyrate production initiated from day 3 at a production rate of 0.6 ± 0.1 g L^{-1} d^{-1} (107.4 ± 19.7g $m^{-2}d^{-1}$), obtaining a titer of 9.2 ± 1.6 g L^{-1} on day 17 before plateauing (Fig. 3). Overall, butyrate was the dominant product with 75.2 ± 1.1 % selectivity. One of the possible reasons for rather stable butyrate concentrations after day 17 of operation was product losses by volatilization during CO_2 sparging, which was reported in our previous work (Yao et al., 2024). The losses became noticeable when the VFAs started to accumulate and reached a certain concentration (ca. 8.8 g L^{-1}). Additionally, trace amounts of caproate were obtained at the end of the experiments, although the final titer remained below 0.3 g L^{-1}.

Each batch cycle was conducted with an average initial methanol/CO_2 ratio of 2.9 ± 0.3. In total, 206.5 ± 6.4 mmol-C (6.6 ± 0.2 g) of methanol were supplied to the MES cell, 87.8 ± 1.8 % of which (181.3 ± 6.4 mmol-C (5.8 ± 0.2 g)) was consumed. In addition, a total of 88.4 ± 8.4 mmol-C (3.9 ± 0.4 g) of CO_2 was utilized throughout the experiments. The average methanol consumption rate was 18.0 ± 0.6 mM d^{-1} (0.58 ± 0.02 g L^{-1} d^{-1}), which was 1.7-fold higher than our previous study (0.32 g L^{-1} d^{-1}) (Yao et al., 2024). Compared to the previous study, where methanol/CO_2 ratio averaged 0.33, this study assessed a ratio of 3, which promoted butyrate production and resulted in the due to the higher availability of reducing equivalents.

Methanol and the cathode electrode were the two electron donors, which collectively provided 3254.5 ± 37.8 mmol equivalents of electrons. Out of these, 42.9 ± 1.9 % were recovered as H_2, 17.9 ± 0.7 % were recovered as butyrate and 6.7 ± 1.0 % were recovered as acetate. In summary, a carbon conversion efficiency of 64.0 ± 5.8 % and a faradaic efficiency of 67.6 ± 3.5 % were obtained (see supplementary information), suggesting further optimization of electron utilization should be done. For example, addition of exogenous electron mediators to improve the electron transfer (Yu et al., 2025), cathode development to enhance the H_2 utilization and thus the biofilm formation (Li et al., 2024b), and reactor design development (Cabau-Peinado et al., 2024) have the potential to improve the faradaic efficiency in MES studies. It is worth mentioning that product losses due to volatilization during gas sparging were not included in the carbon and faradaic efficiency calculations. The OD_{600} of the catholyte at the end of the experiments was only 0.2 (see supplementary information), suggesting that carbon sources were directed to the products, rather than biomass. The butyrate yield obtained was 0.58 ± 0.01 mol-C mol-C^{-1}, indicating a ca. 2-fold enhancement compared to the highest results obtained in serum flasks (0.29 ± 0.02 mol-C mol-C^{-1}).

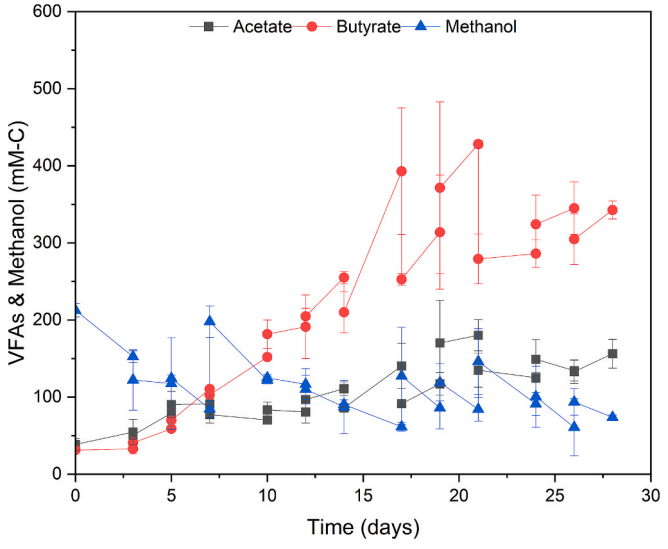

Fig. 3. VFAs and methanol concentrations throughout the MES-35 experiments. Error bars show the standard deviation of duplicate results. Two data points per day represent measurements taken before and after CO_2 sparging. Differences between the two may result from partial loss of volatile fatty acids during sparging, particularly at higher butyrate concentrations.

The highest butyrate production rate obtained in this study, 0.6 g L^{-1} d^{-1} (107.4 g m^{-2} d^{-1}) is close to the highest butyrate production reported from CO_2 in MES studies (Fig. 4.a). Several studies have demonstrated the production of butyrate with only CO_2 supply, although direct elongation of CO_2 to butyrate has not been proven. For example, Jourdin and his co-workers (Jourdin et al., 2019) achieved a high butyrate production rate of 0.7 ± 0.2 g L^{-1} d^{-1}(125 ± 44.9 g m^{-2} d^{-1}) by increasing the CO_2 loading rate (173 L d^{-1}) and high hydraulic retention time (14 d) in continuous feeding mode, which is the highest butyrate production rate reported so far in MES. The high CO_2 loading rate provided excessive amount of carbon for carboxylates production (less than 1 % of the provided carbon was utilized), while the long HRT enabled sufficient time for elongating acetate to butyrate (Jourdin et al., 2019). Raes et al., (2017) added acetate as a co-substrate with CO_2 to facilitate butyrate formation in MES, obtaining a butyrate production rate of 0.54 g L^{-1} d^{-1}. Both studies stated that the most-likely chain elongation route was through ethanol formation, although ethanol was not observed as it was simultaneously produced and consumed.

As suggested by Izadi et al. (2021), butyrate production in MES often requires an additional electron donor apart from H_2. One effective strategy to enhance butyrate production is to promote solventogenesis, thereby increasing the ethanol production in MES. Generally, low pH (below 5) and high P_{H2} (over 1 atm) are favorable for solventogenesis (Romans-Casas et al., 2023). These strategies have been applied in MES to enhance the in-situ ethanol production (Romans-Casas et al., 2024; Vassilev et al., 2019), achieving butyrate production rates of 0.18 g L^{-1} d^{-1} (14.4 g m^{-2} d^{-1}) (Romans-Casas et al., 2024). Other approaches were based on supplying exogenous electron donors, such as ethanol (Izadi et al., 2021; Jiang et al., 2020), formate (Izadi et al., 2021), lactate (Zhang et al., 2023) or methanol (Yao et al., 2024) to support butyrate production in MES. Out of them, ethanol and methanol possess the highest reducing power (degree of reduction 6) compared to formate (1) and lactate (4). Ethanol driven butyrate production in MES was obtained by Zhang et al., (2023), with a butyrate production rate of 0.44 g L^{-1} d^{-1} (44.0 g m^{-2} d^{-1}) by adding 5 g L^{-1} of ethanol at the beginning of the experiment. In the same study, butyrate production rate further increased to 0.9 g L^{-1} d^{-1} (90.0 g m^{-2} d^{-1}) with the addition of both ethanol and lactate (5 g L^{-1} each). Compared to Zhang et al. (2023), similar butyrate production rate of 0.6 g L^{-1} d^{-1} (107.4 g m^{-2} d^{-1}) was obtained in this study by adding similar amounts of methanol (4.6 g L^{-1} of methanol). Compared to our previous study, in which methanol/CO_2 ratios of around 1 were utilized, the butyrate production rate improved by 1.5-fold (as volumetric production rate) or 3.4-fold (normalized to the electrode surface) (Yao et al., 2024). Methanol/CO_2 ratio of 3, pH of 6 (Yao et al., 2025), atmospheric pressure, and 35℃ temperature should be set to enhance butyrate production rate in methanol-assisted MES.

The butyrate selectivity of ca. 80 % achieved in this study with methanol assisted MES is in line with the selectivity obtained in ethanol

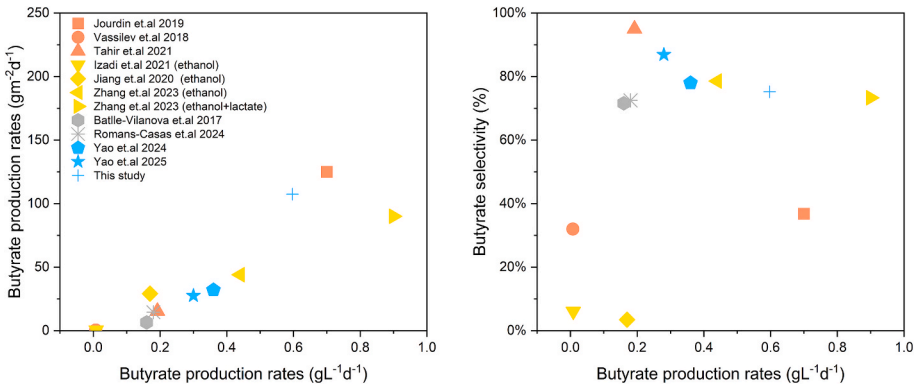

Fig. 4. Comparison of butyrate production rates per projected electrode surface area (a); and butyrate selectivity (b) reported in this study and in other published MES studies (Batlle-Vilanova et al., 2017; Izadi et al., 2021; Jiang et al., 2020; Jourdin et al., 2019; Romans-Casas et al., 2024; Tahir et al., 2021; Vassilev et al., 2018; Yao et al., 2024, 2025; Zhang et al., 2023). Both figures use butyrate production rates normalized to catholyte volume on the x-axis. The figures are split to provide a clearer comparison of the different parameters. Color coding: Orange denotes MES studies without observing ethanol production/consumption. Yellow denotes MES studies with exogenous electron donor addition. Grey denotes MES studies with in-situ ethanol production. Blue denotes methanol assisted MES studies. (For interpretation of the references to color in this figure legend, the reader is referred to the web version of this article.)

assisted MES (Fig. 4, b). However, the highest reported butyrate selectivity in MES (95 %) was obtained with only CO_2 feeding (Tahir et al., 2021). The butyrate selectivity increased from 37 % with unmodified carbon felt to 95 % with the nickel ferrite-coated carbon felt, which suggests that integrating advanced electrode designs with methanol-assisted MES has the potential to further enhance butyrate selectivity while maintaining high production rates.

The two MES validations demonstrated different product spectra in methanol assisted MES. Future studies should focus on microbial community profiling and employ bioinformatics tools, including transcriptomics, metabolomics, and proteomics to better understand the metabolic changes driving these shifts in product distribution.

4. Conclusions

In this study, the effects of different operational parameter combinations on methanol assisted butyrate production via gas fermentation and MES were studied. In gas fermentation experiments, a maximum butyrate yield of 0.29 mol-C mol-C^{-1} was obtained at 35 °C, 1 atm headspace pressure and a methanol/CO_2 ratio of 3. This combination was further validated in fed-batch MES system, obtaining a butyrate production rate of 107.4 ± 19.7 g m^{-2} d^{-1}, with 75.2 ± 1.1 % selectivity. The high methanol/CO_2 ratio enabled efficient methanol utilization at a rate of 0.58 ± 0.02 g L^{-1} d^{-1} and achieved a carbon conversion efficiency of 64.0 ± 5.8 % and faradaic efficiency of 67.6 ± 3.5 %. In summary, a high-rate butyrate production in methanol assisted MES while maintaining high butyrate selectivity was obtained by increasing the methanol/CO_2 ratio. However, excessive methanol concentration in the catholyte (above 250 mM) may hinder the butyrate producing microbial community.

CRediT authorship contribution statement

Hui Yao: Writing – review & editing, Visualization, Methodology, Investigation, Formal analysis, Conceptualization. **Paolo Dessì:** Writing – review & editing, Supervision, Methodology, Funding acquisition. **Meritxell Romans-Casas:** Writing – review & editing, Methodology, Investigation. **Sebastià Puig:** Writing – review & editing, Supervision, Funding acquisition, Conceptualization. **Marika Kokko:** Writing – review & editing, Supervision, Funding acquisition, Conceptualization.

Declaration of competing interest

The authors declare that they have no known competing financial interests or personal relationships that could have appeared to influence the work reported in this paper.

Acknowledgements

The authors acknowledge the funding from Research Council of Finland (grant no. 329227), the Bio and Circular Economy Research Infrastructure (decision no. 353658), and the Finnish cultural foundation (grant no. 241237) and Spanish Ministry of Innovation and Science (ref. PID2021-126240OB-I00). The authors also acknowledge the technical support of Serveis Tècnics de Recerca-Universitat de Girona. S.P. is a Serra Hunter Fellow (UdG-AG-575) and acknowledges the funding from the AGAUR–ICREA Acadèmia Programme, supported by the Department of Research and Universities of the Government of Catalonia. LEQUIA has been recognized as "consolidated research group" (Ref. 2021 SGR01352) by the Catalan Agency of Research and Universities. P.D. acknowledges the support from the project RESTART, funded through the "Dipartimenti di Eccellenza 2023-2027" initiative of the Italian Ministry of University and Research.

Appendix A. Supplementary data

Supplementary data to this article can be found online at https://doi.org/10.1016/j.biortech.2025.133150.

Data availability

Data will be made available on request.

References

Joyia, A.K., M., Ahmad, M., Chen, Y.-F., Mustaqeem, M., Ali, A., Abbas, A., Ashraf Gondal, M.,, 2024. Trends and advances in sustainable bioethanol production technologies from first to fourth generation: a critical review. Energ. Conver. Manage. 321, 119037. https://doi.org/10.1016/j.enconman.2024.119037.

Ale Enriquez, F., Ahring, B.K., 2023. Strategies to overcome mass transfer limitations of hydrogen during anaerobic gaseous fermentations: a comprehensive review. Bioresour. Technol. 377, 128948. https://doi.org/10.1016/j.biortech.2023.128948.

Appel, A.M., Bercaw, J.E., Bocarsly, A.B., Dobbek, H., DuBois, D.L., Dupuis, M., Ferry, J. G., Fujita, E., Hille, R., Kenis, P.J.A., Kerfeld, C.A., Morris, R.H., Peden, C.H.F., Portis, A.R., Ragsdale, S.W., Rauchfuss, T.B., Reek, J.N.H., Seefeldt, L.C., Thauer, R. K., Waldrop, G.L., 2013. Frontiers, Opportunities, and challenges in Biochemical and Chemical Catalysis of CO2 Fixation. Chem. Rev. 113, 6621–6658. https://doi.org/10.1021/cr300463y.

Batlle-Vilanova, P., Ganigué, R., Ramió-Pujol, S., Bañeras, L., Jiménez, G., Hidalgo, M., Balaguer, M.D., Colprim, J., Puig, S., 2017. Microbial electrosynthesis of butyrate from carbon dioxide: Production and extraction. Bioelectrochemistry 117, 57–64. https://doi.org/10.1016/j.bioelechem.2017.06.004.

Cabau-Peinado, O., Winkelhorst, M., Stroek, R., de Angelino, R., K., Straathof, A.J.J., Masania, K., Daran, J.M., Jourdin, L.,, 2024. Microbial electrosynthesis from CO2 reaches productivity of syngas and chain elongation fermentations. Trends Biotechnol. 42, 1503–1522. https://doi.org/10.1016/j.tibtech.2024.06.005.

Chen, W.S., Huang, S., Strik, D.P.B.T.B., Buisman, C.J.N., 2017. Isobutyrate biosynthesis via methanol chain elongation: converting organic wastes to platform chemicals. J. Chem. Technol. Biotechnol. 92, 1370–1379. https://doi.org/10.1002/jctb.5132.

Chen, W.S., Ye, Y., Steinbusch, K.J.J., Strik, D.P.B.T.B., Buisman, C.J.N., 2016. Methanol as an alternative electron donor in chain elongation for butyrate and caproate formation. Biomass Bioenergy 93, 201–208. https://doi.org/10.1016/j.biombioe.2016.07.008.

De Leeuw, K.D., De Smit, S.M., Van Oossanen, S., Moerland, M.J., Buisman, C.J.N., Strik, D.P.B.T.B., 2020. Methanol-based Chain Elongation with Acetate to n-Butyrate and Isobutyrate at Varying Selectivities Dependent on pH. ACS Sustainable Chemistry and Engineering 8, 8184–8194. https://doi.org/10.1021/acssuschemeng.0c00907.

De Smit, S.M., De Leeuw, K.D., Buisman, C.J.N., Strik, D.P.B.T.B., 2019. Continuous n-valerate formation from propionate and methanol in an anaerobic chain elongation open-culture bioreactor. Biotechnol. Biofuels 12, 1–16. https://doi.org/10.1186/s13068-019-1468-x.

Fang, W., Guo, W., Lu, R., Yan, Y., Liu, X., Wu, D., Li, F.M., Zhou, Y., He, C., Xia, C., Niu, H., Wang, S., Liu, Y., Mao, Y., Zhang, C., You, B., Pang, Y., Duan, L., Yang, X., Song, F., Zhai, T., Wang, G., Guo, X., Tan, B., Yao, T., Wang, Z., Xia, B.Y., 2024. Durable CO2 conversion in the proton-exchange membrane system. Nature 626, 86–91. https://doi.org/10.1038/s41586-023-06917-5.

Flaiz, M., Poehlein, A., Wilhelm, W., Mook, A., Daniel, R., Dürre, P., Bengelsdorf, F.R., 2024. Refining and illuminating acetogenic Eubacterium strains for reclassification and metabolic engineering. Microb. Cell Fact. 23, 24. https://doi.org/10.1186/s12934-024-02301-8.

Gaddy, J.L., 1997. Clostridium stain which produces acetic acid from waste gases. Biotechnol. Adv. 15, 563.

Izadi, P., Fontmorin, J.M., Virdis, B., Head, I.M., Yu, E.H., 2021. The effect of the polarised cathode, formate and ethanol on chain elongation of acetate in microbial electrosynthesis. Appl. Energy 283, 116310. https://doi.org/10.1016/j.apenergy.2020.116310.

Jiang, Y., Chu, N., Qian, D.-K., Jianxiong Zeng, R., 2020. Microbial electrochemical stimulation of caproate production from ethanol and carbon dioxide. Bioresour. Technol. 295, 122266. https://doi.org/10.1016/j.biortech.2019.122266.

Jourdin, L., Burdyny, T., 2021. Microbial Electrosynthesis: where do we go from here? Trends Biotechnol. 39, 359–369. https://doi.org/10.1016/j.tibtech.2020.10.014.

Jourdin, L., Winkelhorst, M., Rawls, B., Buisman, C.J.N., Strik, D.P.B.T.B., 2019. Bioresource Technology Reports Enhanced selectivity to butyrate and caproate above acetate in continuous bioelectrochemical chain elongation from CO 2 : Steering with CO 2 loading rate and hydraulic retention tim. Bioresour. Technol. Rep. 7, 100284. https://doi.org/10.1016/j.biteb.2019.100284.

Kim, J.-Y., Park, S., Jeong, J., Lee, M., Kang, B., Jang, S.H., Jeon, J., Jang, N., Oh, S., Park, Z.-Y., Chang, I.S., 2021. Methanol supply speeds up synthesis gas fermentation by methylotrophic-acetogenic bacterium, Eubacterium limosum KIST612. Bioresour. Technol. 321, 124521. https://doi.org/10.1016/j.biortech.2020.124521.

Koskue, V., Rinta-Kanto, J.M., Freguia, S., Ledezma, P., Kokko, M., 2021. Optimising nitrogen recovery from reject water in a 3-chamber bioelectroconcentration cell. Sep. Purif. Technol. 264, 118428. https://doi.org/10.1016/j.seppur.2021.118428.

Kremp, F., Müller, V., 2021. Methanol and methyl group conversion in acetogenic bacteria: biochemistry, physiology and application. FEMS Microbiol. Rev. 45, fuaa040. https://doi.org/10.1093/femsre/fuaa040.

Lee, H., Park, N., Kong, T.-H., Kwon, S., Shin, S., Cha, S.G., Lee, E., Cha, J., Sultan, S., Kwon, Y., 2024. Advancements in electrochemical methanol synthesis from CO2: Mechanisms and catalyst developments. Nano Energy 130, 110099. https://doi.org/10.1016/j.nanoen.2024.110099.

Li, F., Li, Y., Cao, J., Carvalho, L., Lundgren, J., Engvall, K., Zhang, X., Liu, Y., Ji, X., 2024a. Combination of CO2 electrochemical reduction and biomass gasification for producing methanol: a techno-economic assessment. Energ. Conver. Manage. 307, 118380. https://doi.org/10.1016/j.enconman.2024.118380.

Li, S., Kim, M., Song, Y.E., Hwan Son, S., Kim, H., Jae, J., Yan, Q., Fei, Q., Kim, J.R., 2024b. Housing of electrosynthetic biofilms using a roll-up carbon veil electrode increases CO2 conversion and faradaic efficiency in microbial electrosynthesis cells. Bioresour. Technol. 393, 130157. https://doi.org/10.1016/j.biortech.2023.130157.

Nevin, K.P., Woodard, T.L., Franks, A.E., Summers, Z.M., Lovley, D.R., 2010. Microbial electrosynthesis: feeding microbes electricity to convert carbon dioxide and water to multicarbon extracellular organic compounds. MBio 1, e00103.

Oswald, F., Stoll, I.K., Zwick, M., Herbig, S., Sauer, J., Boukis, N., Neumann, A., 2018. Formic Acid Formation by Clostridium ljungdahlii at Elevated pressures of Carbon Dioxide and Hydrogen. Front. Bioeng. Biotechnol. 6. https://doi.org/10.3389/fbioe.2018.00006.

Raes, S.M.T., Jourdin, L., Buisman, C.J.N., Strik, D.P.B.T.B., 2017. Continuous Long-Term Bioelectrochemical Chain Elongation to Butyrate. ChemElectroChem 4, 386–395. https://doi.org/10.1002/celc.201600587.

Ragsdale, S.W., Pierce, E., 2008. Acetogenesis and the Wood–Ljungdahl pathway of CO2 fixation. Biochimica et Biophysica Acta (BBA) - Proteins and Proteomics 1784, 1873–1898. doi:10.1016/j.bbapap.2008.08.012.

Ren, W., He, P., Zhang, H., Lü, F., 2024. Temperature is an underestimated parameter to regulate the start-up of enhanced carbon chain elongation. Renew. Energy 234, 121221. https://doi.org/10.1016/j.renene.2024.121221.

Rode, L.M., Genthner, B.R.S., Bryant, M.P., 1981. Syntrophic association by cocultures of the methanol- and CO2-H2-utilizing species Eubacterium limosum and pectin-fermenting Lachnospira multiparus during growth in a pectin medium. Appl. Environ. Microbiol. 42, 20–22. https://doi.org/10.1128/aem.42.1.20-22.1981.

Romans-Casas, M., Feliu-Paradeda, L., Tedesco, M., Hamelers, H.V., Bañeras, L., Balaguer, M.D., Puig, S., Dessì, P., 2024. Selective butyric acid production from CO2 and its upgrade to butanol in microbial electrosynthesis cells. Environ. Sci. Ecotechnol. 17, 100303.

Romans-Casas, M., Perona-Vico, E., Dessì, P., Bañeras, L., Balaguer, M.D., Puig, S., 2023. Boosting ethanol production rates from carbon dioxide in MES cells under optimal solventogenic conditions. Sci. Total Environ. 856, 159124. https://doi.org/10.1016/j.scitotenv.2022.159124.

Sharak Genthner, B.R., Bryant, M.P., 1987. Additional characteristics of one-carbon-compound utilization by Eubacterium limosum and Acetobacterium woodii. Appl. Environ. Microbiol. 53, 471–476.

Shin, J., Bae, J., Lee, H., Kang, S., Jin, S., Song, Y., Cho, S., Cho, B.-K., 2023. Genome-wide CRISPRi screen identifies enhanced autolithotrophic phenotypes in acetogenic bacterium Eubacterium limosum. Proc. Natl. Acad. Sci. 120, e2216244120. https://doi.org/10.1073/pnas.2216244120.

Skidmore, B.E., Baker, R.A., Banjade, D.R., Bray, J.M., Tree, D.R., Lewis, R.S., 2013. Syngas fermentation to biofuels: Effects of hydrogen partial pressure on hydrogenase efficiency. Biomass Bioenergy 55, 156–162. https://doi.org/10.1016/j.biombioe.2013.01.034.

Tabibian, S.S., Sharifzadeh, M., 2023. Statistical and analytical investigation of methanol applications, production technologies, value-chain and economy with a special focus on renewable methanol. Renew. Sustain. Energy Rev. 179, 113281. https://doi.org/10.1016/j.rser.2023.113281.

Tahir, K., Miran, W., Jang, J., Woo, S.H., Lee, D.S., 2021. Enhanced product selectivity in the microbial electrosynthesis of butyrate using a nickel ferrite-coated biocathode. Environ. Res. 196, 110907. https://doi.org/10.1016/j.envres.2021.110907.

Taylor, I.J., Senior, P.J., 1978. Single cell proteins: a new source of animal feeds. Endeavour 2, 31–34. https://doi.org/10.1016/0160-9327(78)90031-5.

Van Hecke, W., Bockrath, R., De Wever, H., 2019. Effects of moderately elevated pressure on gas fermentation processes. Bioresour. Technol. 293, 122129. https://doi.org/10.1016/j.biortech.2019.122129.

Varela, H., Paredes-Salazar, E.A., Lima, F.H.B., Eid, K., 2024. Renewable methanol and the energy challenge: The role of electrocatalysis. Current Opinion in Electrochemistry 46, 101539. https://doi.org/10.1016/j.coelec.2024.101539.

Vassilev, I., Hernandez, P.A., Batlle-Vilanova, P., Freguia, S., Krömer, J.O., Keller, J., Ledezma, P., Virdis, B., 2018. Microbial Electrosynthesis of Isobutyric, Butyric, Caproic Acids, and corresponding Alcohols from Carbon Dioxide. ACS Sustainable Chemistry and Engineering 6, 8485–8493. https://doi.org/10.1021/acssuschemeng.8b00739.

Vassilev, I., Kracke, F., Freguia, S., Keller, J., Krömer, J.O., Ledezma, P., Virdis, B., 2019. Microbial electrosynthesis system with dual biocathode arrangement for simultaneous acetogenesis, solventogenesis and carbon chain elongation. Chem. Commun. https://doi.org/10.1039/c9cc00208a.

von Canstein, H., Ogawa, J., Shimizu, S., Lloyd, J.R., 2008. Secretion of Flavins by Shewanella Species and their Role in Extracellular Electron transfer. Appl. Environ. Microbiol. 74, 615–623. https://doi.org/10.1128/AEM.01387-07.

Wendlandt, K.-D., Jechorek, M., Brühl, E., 1993. The influence of pressure on the growth of methanotrophic bacteria. Acta Biotechnol. 13, 111–115. https://doi.org/10.1002/abio.370130205.

Wood, J.C., Marcellin, E., Plan, M.R., Virdis, B., 2022. High methanol-to-formate ratios induce butanol production in Eubacterium limosum. J. Microbial. Biotechnol. 15, 1542–1549. https://doi.org/10.1111/1751-7915.13963.

Yang, H.-Y., Bao, B.-L., Liu, J., Qin, Y., Wang, Y.-R., Su, K.-Z., Han, J.-C., Mu, Y., 2018. Temperature dependence of bioelectrochemical CO2 conversion and methane production with a mixed-culture biocathode. Bioelectrochemistry 119, 180–188. https://doi.org/10.1016/j.bioelechem.2017.10.002.

Yang, H.-Y., Hou, N.-N., Wang, Y.-X., Liu, J., He, C.-S., Wang, Y.-R., Li, W.-H., Mu, Y., 2021. Mixed-culture biocathodes for acetate production from CO2 reduction in the microbial electrosynthesis: Impact of temperature. Sci. Total Environ. 790, 148128. https://doi.org/10.1016/j.scitotenv.2021.148128.

Yao, H., Rinta-Kanto, J.M., Vassilev, I., Kokko, M., 2024. Methanol as a co-substrate with CO2 enhances butyrate production in microbial electrosynthesis. Appl. Microbiol. Biotechnol. 108, 372. https://doi.org/10.1007/s00253-024-13218-y.

Yao, H., Romans-Casas, M., Vassilev, I., Rinta-Kanto, J.M., Puig, S., Rissanen, A.J., Kokko, M., 2025. Selective butyrate production from CO2 and methanol in microbial electrosynthesis - influence of pH. Bioelectrochemistry 109000. https://doi.org/10.1016/j.bioelechem.2025.109000.

Yasin, M., Jeong, Y., Park, S., Jeong, J., Lee, E.Y., Lovitt, R.W., Kim, B.H., Lee, J., Chang, I.S., 2015. Microbial synthesis gas utilization and ways to resolve kinetic and mass-transfer limitations. Bioresour. Technol. 177, 361–374. https://doi.org/10.1016/j.biortech.2014.11.022.

Yerushalmi, L., Volesky, B., Szczesny, T., 1985. Effect of increased hydrogen partial pressure on the acetone-butanol fermentation by Clostridium acetobutylicum. Appl. Microbiol. Biotechnol. 22, 103–107. https://doi.org/10.1007/BF00250028.

Yu, Y., Shi, Z., Li, W., Bian, M., Cheng, C., Xi, Y., Yao, S., Zeng, X., Jia, Y., 2025. Application of exogenous electron mediator in fermentation to enhance the production of value-added products. Appl. Environ. Microbiol. 91, e00495–e00525. https://doi.org/10.1128/aem.00495-25.

Zhang, K., Qiu, Z., Luo, D., Song, T., Xie, J., 2023. Hybrid electron donors of ethanol and lactate stimulation chain elongation in microbial electrosynthesis with different inoculants. Renew. Energy 202, 942–951. https://doi.org/10.1016/j.renene.2022.11.123.

Zhao, T., Li, Y., Zhang, Y., 2021. Biological carbon fixation: a thermodynamic perspective. Green Chem. 23, 7852–7864. https://doi.org/10.1039/D0GC03493B.